Interference between four-wave and six-wave mixing in resonant coherent scattering from biexcitons in CuCl

D. S. Chemla
Bell Laboratories, Holmdel, New Jersey 07733

A. Maruani and F. Bonnouvrier
Centre National d'Etudes des Télécommunications, 92200 Bagneux, France

(Received 4 June 1982)

We present the first evidence of interference between four- and six-wave mixing in multiple coherent scattering near the two-photon resonance of biexcitons in CuCl. The experimental data are quantitatively explained by taking proper account of propagation effects and by a model for $\chi^{(5)}$ involving no adjustable parameters.

In a series of previous papers[1–6] we have investigated in detail the resonant forward degenerate four-wave mixing associated with biexcitons in semiconductors. Using an exact analytical solution of the propagation problem[5] which accounts for linear as well as for nonlinear refractive indices and absorption, we have demonstrated the autoionizing character of biexcitons[3] and we have derived some important parameters of the exciton-biexciton system,[6] including the exciton-biexciton oscillator strength f_{xx2}, the biexciton energy W_{x2} and linewidth Γ_{x2}, and the Fano parameter q. The very large efficiency of the process is due to two factors: its nearly triply resonant character and the huge values for f_{xx2}. As a result, in the mutual nonlinear scattering of two laser beams crossing at a small angle in a thin CuCl sample, up to five positive or negative diffraction orders are easily observed with the naked eye, even at such moderate intensities as 1.5 MW/cm^2. They correspond to the following wave vectors and frequencies:

$$k_N^{+} = (N+1)k_p - Nk_t \ ,$$

$$k_N^{-} = (N+1)k_t - Nk_p \ ,$$

$$\omega_N^{\pm} = \omega_p = \omega_t = \omega \ .$$

Here N indicates the order of diffraction, and the subscripts p and t label the pump and the test beams. Note that for $N=5$ the scattering corresponds to a 12 photon process.

Since the binding energy of the excitonic molecule is rather large in this compound,[6] there is no change in the diagonal elements of the density matrix. Thus the multiple scatterings are not associated with the usual exciton or free-carrier population-induced gratings. These observations raise the following questions: (1) What are the processes responsible for the mixing? (ii) What are the effective nonlinearities which drive them?

These questions are related to the problems of high-order susceptibilities of the material and to renormalized optical functions.[7] We shall focus the analysis on the first and the second positive order which are diffracted in the directions k_1^{+} and k_2^{+}. Because the highly nonlinear response of the system causes both the line shapes and the position of the extrema to be intensity dependent,[4] it is necessary to eliminate the possible variations in the focused laser intensities or in the location of the excited zone from one run to another. This is performed by a computer controlled experiment which enables us to record simultaneously the intensities I_1 and I_2 and to compute, at each wavelength, the ratio $\rho = I_2/I_1$. An example of our experimental data is shown in Fig. 1 for a CuCl sample 90 μm thick.

The field scattered in the first order, E_1, is generated by a four-wave mixing through the nonlinear polarization (NLP) $P_{\mathrm{NL}}(1) = 3\epsilon_0 \chi^{(3)} E_p^2 E_t^*$. For the field diffracted in the second order, E_2, the most efficient

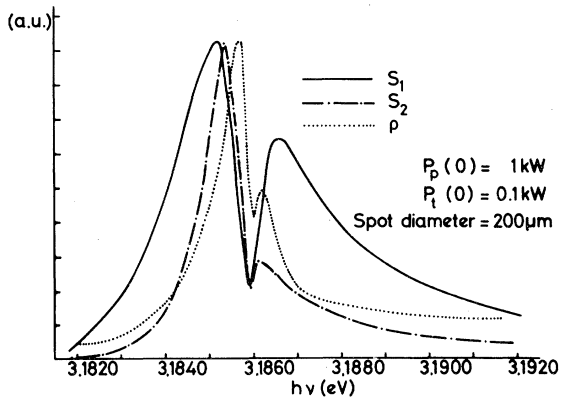

FIG. 1. Experimental data for a 90-μm CuCl sample. The spectra show the variations of the intensities of the first- and second-order diffracted beams I_1(——) and I_2(—·—·). The dotted line (· · · ·) corresponds to the experimental ratio $\rho = I_2/I_1$.

processes of generation occur through the following NLP's: a component of direct six-wave mixing

$$P_{\mathrm{NL}}^{D}(2)=10\epsilon_0\chi^{(5)}E_p^3E_t^{*2}\ ; \tag{1a}$$

a component of four-wave mixing in cascade, involving E_1 once

$$P_{\mathrm{NL}}^{C1}(2)=6\epsilon_0\chi^{(3)}E_1E_pE_t^*\ ; \tag{1b}$$

a component of four-wave mixing in cascade involving E_1 twice

$$P_{\mathrm{NL}}^{C2}(2)=3\epsilon_0\chi^{(3)}E_1^2E_p^*\ . \tag{1c}$$

These processes are illustrated in the insert of Fig. 2.

Near the two-photon resonance (TPR), the direct process is *a priori* favored in very thin samples, but in that case the intensity of the signal is correspondingly very low. Far from resonance, the parametric approximation indicates that, as in stimulated Raman scattering, cascades are the most efficient processes. For sufficiently thick samples (50–100 μm) and near the TPR, all the processes are involved. Discrimination among them can only be accomplished with a proper propagation analysis and a model for $\chi^{(5)}$.

Let us first consider the problem of propagation for frequencies near the TPR. The coupling between E_p, E_t, and E_1 has been discussed at length in Refs. 5 and 6. For the case that pump depletion due to the generation of E_1 is negligible relative to pump-induced two-photon absorption. An analytical solution for $E_p(z)$, $E_t(z)$, and $E_1(z)$ has been given previously.[5,6] It was checked versus the full numerical solution, and it proved to describe accurately the experimental data, even at resonance, provided that $I_p \gtrsim 5I_t$.[5]

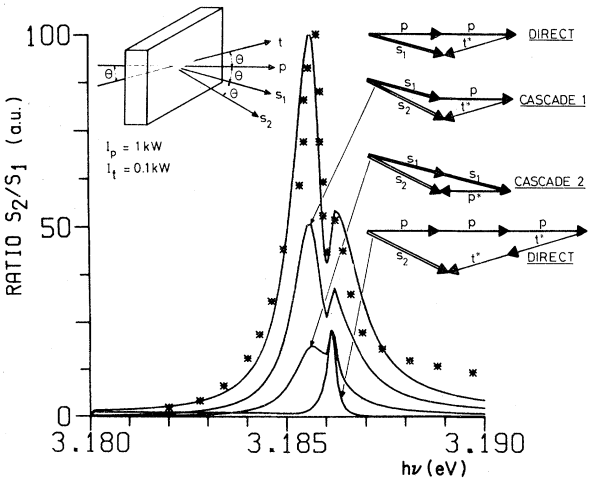

FIG. 2. Comparison of the experimental data for ρ (asterisks) with the prediction of the model; no adjustable parameter are involved. The four processes contributing to the scattering are illustrated in the inset.

The propagation equation for E_N is written

$$\frac{d}{dz}E_N+(\tfrac{1}{2}\alpha+A_N)E_N=G_N\ . \tag{2}$$

Here $A_N\propto(\chi^{(3)}|E_j|^2+\chi^{(5)}|E_j|^2|E_l|^2+\cdots)$ describes the nonlinear absorption and phase-shift while G_N describes the nonlinear gain of corresponding order. Now a key point is that for $I_p \gg I_t$ the A_N terms are the same for all the fields E_N (namely, pump induced). Thus they all experience the same linear absorption and the same (pump-induced) nonlinear absorptions and phase shifts. Hence the ratios $E_N/E_{N'}$ depend on only the gain terms G_N and $G_{N'}$ and are easier to analyze. For instance the propagation equation of $r=E_2/E_1=\rho^{1/2}\exp(i\phi)$ becomes

$$E_1\frac{d}{dz}r+G_1r=G_2\ , \tag{3}$$

where $G_1=i(\omega/2\epsilon_0nc)P_{\mathrm{NL}}(1)$ and $G_2=G_2^D+G_2^{C1}+G_2^{C2}$. The individual gain components correspond to the three NLP of Eqs. (1a), (1b), and (1c);

$$G_2^D=i\frac{10\omega}{2nc}\chi^{(5)}E_p^3E_t^{*2}\ ,$$

$$G_2^{C1}=i\frac{6\omega}{2nc}\chi^{(3)}\left(1+10\frac{\chi^{(5)}}{\chi^{(3)}}|E_p|^2\right)E_1E_pE_t^*\ ,$$

$$G_2^{C2}=i\frac{3\omega}{2nc}\chi^{(3)}\left(1+10\frac{\chi^{(5)}}{\chi^{(3)}}|E_p|^2\right)E_1^2E_p^*\ .$$

These must be developed consistently to the same order in E_p. Using the analytical solution for $E_p(z)$, $E_t(z)$, and $E_1(z)$ in the linear Eq. (3) it is possible to obtain a very fast integration for r.

To attempt any comparison with the experimental data it is necessary to have a model for $\chi^{(5)}$. In the three-level system (ground state g, exciton x, and biexciton $x2$), the exciton-biexciton transition is much more probable than the others ($f_{xx2}\gtrsim 10^3 f_{gx}$; $f_{gx2}=0$). Retaining the dominant terms in the three first susceptibilities one has[1]

$$\chi^{(5)}=\tfrac{3}{4}(\chi^{(3)})^2/\chi^{(1)}\ . \tag{4}$$

This equation is valid even if the biexciton is an autoionizing level,[3,6] i.e.,

$$\chi^{(3)}\propto f_{gx}f_{xx2}(W_x-\hbar\omega-i\Gamma_x)^{-2}(W_{x2}-2\hbar\omega-i\Gamma_{x2})^{-1}$$
$$\times[1-2iq^{-1}+i(W_{x2}-2\hbar\omega)/q^2\Gamma_{x2}]\ .$$

In CuCl, $\chi^{(1)}$ is given by the linear optical properties of the exciton and $\chi^{(3)}$ is known unambiguously from our previous work[6]: $\chi^{(5)}$ is thus fixed *without any adjustable parameter.*

Our experimental data of Fig. 1 (asterisks) are compared to the model calculation in Fig. 2. The four solid lines correspond to the solution for G_2^D,

G_2^{C1}, G_2^{C2}, and $G_2 = G_2^D + G_2^{C1} + G_2^{C2}$. They do not represent a fit, since all the parameters are known. Excellent agreement is obtained when the coherent sum of the three components, i.e., G_2 is used. This agreement allows the following comments:

(a) The leading mechanism below the TPR is the C1 cascade process, which drives the intensity and the line shape of the signal, but close to resonance the direct process contributes $\simeq 30\%$ of the total signal: Six-photon mixing is evidenced through this spectroscopy. It is unambiguous that the three processes interfere, since the total intensities below and above the TPR are, respectively, 1.4 and 0.67 times the sum of the intensities corresponding to the individual processes. This is a very strong test of the model, since it proves that the behavior of the relative phases of G_2^D, G_2^{C1}, and G_2^{C2} is correctly described across the TPR. The dissymmetry between the two sides of the TPR is induced by the autoionizing character of biexcitons.[3,6]

(b) Renormalization is important: The dimensionless factor $\chi^{(5)}|E_p|^2/\chi^{(3)}$ is a highly structured complex number; although its effects contribute only to a few percent of the intensity, they affect the line shapes qualitatively.

(c) The autoionizing character is qualitatively and quantitatively confirmed: All calculations with values for q differing from $q = 15 \pm 1$ (Refs. 3 and 6) give a poorer agreement with experiment.

The line shape is extremely intensity dependent as shown by the three-dimensional plot in Fig. 3 which represents the calculated ρ as a function of the initial pump intensity $I_p(0)$ and the photon energy $h\nu$. All the curves in this plot agree very well with the corresponding experiments.

In conclusion, we have shown that close to a biexciton TPR high-order nonlinear processes contribute to the dielectric response of semiconductors. They are evidenced both by a direct six-wave process and through the renormalization of lower-order susceptibilities.[7] We have successfully accounted for the experimental data by a model involving no adjustable parameters.

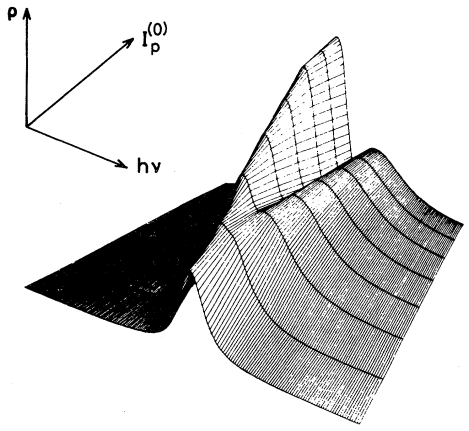

FIG. 3. Three-dimensional plot of the ratio $\rho = I_2/I_1$ as a function of the photon energy ($3.18 \lesssim h\nu \lesssim 3.188$ eV) near the two-photon resonance $\frac{1}{2}W_{x2} = 3.186$ eV, and of the pump intensity (7.5 kW/cm$^2 \lesssim I_p \lesssim 2.75$ MW/cm^2).

A more detailed presentation of our experimental work and a more lengthy discussion of its interpretation are planned to be presented elsewhere.

Edmond Batifol is warmly thanked for his extensive and skillful contribution to the experimental work.

[1]A. Maruani, J. L. Oudar, E. Batifol, and D. S. Chemla, Phys. Rev. Lett. 41, 1372 (1978).
[2]J. L. Oudar, A. Maruani, E. Batifol, and D. S. Chemla, J. Opt. Soc. Am. 68, 11 (1978).
[3]D. S. Chemla, A. Maruani, and E. Batifol, Phys. Rev. Lett. 42, 1075 (1979).
[4]A. Maruani and D. S. Chemla, J. Phys. Soc. Jpn. 49, 585 (1980).
[5]A. Maruani, IEEE J. Quantum Electron. 16, 558 (1980).
[6]A. Maruani and D. S. Chemla, Phys. Rev. B 23, 841 (1981).
[7]S. W. Koch and H. Haug, Phys. Rev. Lett. 46, 450 (1981).